Coexistence of alleles: insights of Modern Coexistence Theory into the maintenance of genetic diversity

Alba Cervantes-Loreto[1], Michelle L. Maraffini[1], Daniel B. Stouffer[1], and Sarah P. Flanagan[1]

[1]Centre for Integrative Ecology, School of Biological Sciences, University of Canterbury, Christchurch 8140, New Zealand

---

Words in abstract	to be determined
Words in manuscript	to be determined
Number of references	to be determined
Number of figures	to be determined
Number of tables	2
Number of text boxes	0
Corresponding author	Alba Cervantes-Loreto
Phone	+64 369 2880
Email	alba.cervantesloreto@pg.canterbury.ac.nz

---

1 Introduction

The question of how genetic variation is maintained, despite the effects of selection and drift, continues to be central to the study of evolutionary biology (Walsh & Lynch, 2018). Classical explanations include overdominance (heterozygote advantage) or frequency-dependent selection, but in the modern era of genomic data, all patterns of variation that exceed the expected variation under neutrality tend to be categorized broadly as balancing selection, regardless of the evolutionary mechanism (Mitchell-Olds *et al.*, 2007). One of the evolutionary mechanisms coined under balancing selection is sexually antagonistic selection, which occurs when the direction of natural selection on traits or loci differs between the sexes (Connallon & Hall, 2018).

Sexually antagonistic selection has been identified as a powerful engine of speciation that in some cases can mantain polymorphisms of otherwise dis-advantageous alleles in a population (Gavrilets, 2014). The effect of sexually antagonistic selection, however, has been generally studied under strong simplifying assumptions such as constant population sizes and homogeneous environments (e.g.,Kidwell *et al.* (1977); Pamilo (1979); Immler *et al.* (2012)). Few studies have explored the effect of sexually antagonistic selection on the maintenance of polymorphism with more realistic assumptions. Excepctions include Connallon *et al.* (2018) who found that classical predictions break down when fluctuations in the environment combined with life-history traits allow local adaptations and promote the maintenance of genetic diversity. The effect of environmental fluctuations without local adaptation, however, has not been studied in the context of sexually

antagonistic selection to the best of our knowledge.

The contribution of environmental fluctuations to genetic variability remains a debated issue in evolutionary biology. Classic theoretical models predict that temporal fluctuations in environmental conditions are unlikely to maintain a genetic polymorphism (Hedrick, 1974; 1986). However, other studies have found that fluctuating selection can maintain genetic variance on sex–linked traits (Reinhold, 2000), or in populations where generations overlap (Ellner & Hairston Jr, 1994; Ellner & Sasaki, 1996). Similarly, temporal changes in population sizes have been shown to mitigate the effect of genetic drift in small populations (Pemberton *et al.*, 1996), and in annual plant systems (Nunney, 2002). Thus, both fluctuations in selection and population sizes could dramatically change the effect of sexually antagonistic selection in the maintenance of genetic diversity.

Importantly, progress requires more than just identifying if fluctuations can maintain genetic diversity in a population, but to quantify how exactly they contribute to its maintenance (Ellner *et al.*, 2016). Modern coexistence theory (MCT) provides a powerful conceptual framework to do so (Chesson, 2000b; 1994; Barabás *et al.*, 2018). Although its core ideas were formalized in an ecological context (Chesson, 1994; 2000a), this framework provides the necessary tools to examine the relative contributions of fluctuations to diversity maintenance, which can also be applied to evolutionary contexts (Ellner & Sasaki, 1996; Reinhold, 2000). From an ecological perspective, polymorphism of sexually antagonistic alleles is equivalent to the coexistence of species, and the fixation of either one of the alleles in a population is equivalent to competitive exclusion. The coexistence of alleles, thus, can be examined through the same lens as the coexistence of competing species.

Here, we seek to explicitly apply recent advances in MCT to the question of how polymorphism is maintained under sexually antagonistic selection. We examined how fluctuations in selection values, fluctuations in population sizes, and their interactions can stabilize or hinder the coexistence of alleles. In particular, we examined i) Can fluctuations in population sizes and selection values allow sexually antagonistic alleles to coexist when differences in their fitness would typically not allow them to? and ii) What is the relative contribution of different types of fluctuations that allow two sexually antagonistic alleles to be maintained in a population? Our study provides the tools to analyze evolutionary dynamics from a novel perspective and contributes to answering long-lasting questions regarding the effect of non-constant environments on genetic diversity.

2 Methods

We first present a model that describes the evolutionary dynamics of sexually antagonistic alleles and show how changes in allele frequencies can be expressed in terms of growth rates, a necessary condition for analyses done using MCT. We continue by simulating different scenarios of alleles invading a population, where we allowed population sizes, selection values, both, or neither to vary. Finally, we examine the results of our simulations through a MCT lens by calculating the contribution of each of these fluctuations in the coexistence of alleles across the parameter space of sexually antagonistic selection.

Population dynamics of sexually antagonistic alleles

As most population genetic models of sex-dependent selection, our model considered evolution at single, biallelic locus with frequency and density independent effects on the relative fitness of females and males (Wright, 1942; Kidwell *et al.*, 1977; Immler *et al.*, 2012). We examined the dynammics of two sexually antagonistic alleles, j and k, that affect fitness in the haploid state. We assumed allele j always has a high fitness in females ($w_{jf} = 1$), but variable fitness in males ($w_{jm} < 1$); and allele k has a high fitness in males ($w_{km} = 1$), but variable fitness in females ($w_{kf} < 1$). The selection against allele j in males is therefore $S_m = 1 - w_{jm}$, and the selection against allele k in females is $S_f = 1 - w_{kf}$.

ACL: Add more recent refs, sarahs suggestions and e.g.,

The frequency of each allele in each sex at the beginning of a life-cycle at time t is given by:

$$p_{jm,t} = \frac{n_{jm,t}}{N_{m,t}} \tag{1}$$

$$p_{jf,t} = \frac{n_{jf,t}}{N_{f,t}} \tag{2}$$

$$p_{km,t} = \frac{N_{m,t} - n_{jm,t}}{N_{m,t}} \tag{3}$$

$$p_{kf,t} = \frac{N_{f,t} - n_{jf,t}}{N_{f,t}} \tag{4}$$

where $N_{m,t}$ and $N_{t,t}$ are the numbers of males and females in a population at time t, $n_{jf,t}$ is the number of females f with allele j, and $n_{jm,t}$ is the number of males m with allele j at time t, respectively.

The individuals in the population mate at random before selection occurs, and there-

fore the frequency of offspring with allele j after mating, $p'_{j,t}$ can be expressed as:

$$p'_{j,t} = \frac{(N_{m,t} n_{jf,t} + N_{f,t} n_{jm,t})}{2 N_f N_m} \,. \tag{5}$$

Selection acts upon these offspring in order to determine the allelic frequencies in females and males in the next generation, $t+1$. As an example the frequency of females with allele j after selection is given by:

$$p'_{jf,t+1} = \frac{n_{jf,t+1}}{N'_{f,t+1}} = \frac{p'_j w_{jf}}{p'_j w_{jf} + (1 - p'_j) w_{kf}} \tag{6}$$

The logarithmic growth rate of j in females, is therefore given by the number of females with allele j after selection, divided by the original number of females carrying allele j:

$$r_{jf,t} = \ln \left(\frac{n'_{jf,t+1}}{n_{jf,t}} \right) \tag{7}$$

An equivalent expression for the per capita growth rate of allele j in males m can be obtained by exchanging f for m across the various subscripts in this expression.

Allelic coexistence in a sexual population, however, is ultimately influenced by growth and establishment of an allele across both sexes. Therefore, the full growth rate of allele j across the entire population of females *and* males is given by:

$$r_j = \ln \left(\frac{n'_{jf,t+1} + n'_{jm,t+1}}{n_{jf,t} + n_{jf,t}} \right) \,. \tag{8}$$

An equivalent expression describes r_k, the growth rate of allele k.

Selection mantains both alleles in the population under the condition that:

$$\frac{S_m}{1+S_m} < S_f < \frac{S_m}{1-S_m} \tag{9}$$

Thus,the maintenance of polymorphism of sexually antagonistic alleles is solely determined by the values of S_m and S_f. Note that in our model, the values S_m and S_f can take are bounded from 0 to 1. Therefore the parameter space of sexually antagonistic selection is within the range $0 < S_m, S_f < 1$. Classic theoretical models predict that in constant environments, only in ≈ 0.38 of the selection parameter space alleles can coexist (Kidwell *et al.*, 1977; Pamilo, 1979; Connallon *et al.*, 2018). If fluctuations in population sizes or selection values have an effect on the coexistence of sexually antagonistic alleles, it would be reflected in increases or decreases of the proportion of the parameter space of selection where polymorphism is maintained.

Simulations

Typically, MCT would require decomposing alleles' growth rates (e.g., Eqn. 8) analytically to examine the relative contributions of different types of fluctuations to their coexistence (Barabás *et al.*, 2018). Although we present an analytical approach in the Supporting Information, our general solution is not easily interpretable and soon becomes mathematically intractable (S1 Supporting Information). Thus, we opted for an extension of MCT that provides the flexibility to examine the contributions of different processes to coexistence using simulations (Ellner *et al.*, 2019; Shoemaker *et al.*, 2020).

For each simulation, we examined coexistence outcomes across the selection parameter space of sexually antagonistic selection ($0 < S_m, S_f < 1$). To do so, we partitioned the parameter space into a grid of 50×50, which yielded 2500 pairwise combinations of different w_{jm} and w_{kf} values. For each pairwise combination of w_{jm} and w_{kf}, as we detail in the next sections, we iterated our model while controlling the effect size of fluctuations in fitness values (σ_w), fluctuations in population sizes (σ_g) and their correlations (ρ_w and ρ_g respectively). Then, we performed simulations of each allele invading a population, determined coexistence outcomes, and the relative contribution of each type of fluctuation. Finally, we calculated for each simulation, the proportion of the parameter space that allowed alleles to coexist.

We explored all of the combinations of low , intermediate and high fluctuations in fitness values and population sizes, with different extents of correlations between fluctuations (Table 1). As a control simulation, we set $\sigma_w = 0.001$ and $\sigma_g = 0.001$, with no correlation between fluctuations. For each one of the factorial combinations of σ_g, σ_w, ρ_g and ρ_w (Table 1), we performed invasion simulations across the parameter space of selection. We ran ten replicates per parameter combination, which resulted in 3780 simulations.

Timeseries

To incorporate the effects of fluctuations into our population dynamics model we generated independent timeseries of fluctuations in fitness values and population sizes. In the case of fluctuations in selection values, for a given value of w_{jm} and w_{kf} (i.e., a fixed point in the selection parameter space), we generated a timeseries of 500 timesteps made

up of correlated fluctuations of w_{jm} and w_{kf}. We controlled the effect size of fluctuations in fitness values (σ_w) and its correlation (ρ_w) by using the Cholesky factorization of the variance-covariance matrix:

$$C_w = \begin{bmatrix} \sigma_w^2 & \rho_w \sigma_w^2 \\ \rho_w \sigma_w^2 & \sigma_w^2 \end{bmatrix} \tag{10}$$

We multiplyed Eqn. 10 by a (2×500) matrix of random numbers from a normal distribution with mean 0 and unit variance, which yielded γ_j and γ_k. Then, we calculated the value of w_{jm} at time $t+1$ as $w_{jm,t+1} = w_{jm}^{\gamma_{j,t}}$. We calculated the value of $w_{kf,t+1}$ analogously.

Similarly, we generated a timeseries of 500 timesteps made up of correlated fluctuations in population sizes. We chose values of N_m and N_f of 200 individuals each as the initial value of population sizes throughout our simulations. We performed a Cholesky factorization of the variance-covariance matrix, controlling the effect size of fluctuations in population sizes with σ_g and their correlation with ρ_g. Similar to our previous approach, we multiplied this factorization by a random matrix of uncorrelated random variables, which yielded γ_m and γ_f. Finally, we calculated the number of males in the population at time $t+1$ as $N_{m,t+1} = N_m + \gamma_{m,t}$. We calculated the value of $N_{f,t+1}$ analogously. Note that the scales of σ_g and σ_w are different from each other. While σ_w controls the exponential change in fitness values in each timestep, σ_g controls the number of individuals added to a population in each timestep. We bounded the values population sizes could take so there were no negative population sizes, since that would not be biologically plausible.

We did not impose an upper bound to the values population sizes could take.

Finally, we performed simulations where our population dynamics model (Eqns. 1 to 8) iterated over 500 timesteps while allowing selection values and population sizes to fluctuate in each timestep. We started each simulation with the initial values of N_m and N_f described before and equal frequencies of allele j and allele k in each sex. For each timestep t in our simulations, the values of w_{jm} w_{kf}, N_m and N_f used to calculate allele´s frequencies in in timestep t (e.g., Eqn. 6), corresponded to the t values calculated in each timeseries, as described previously. This approach yielded a final timeseries that captured the dynamics of sexually antagonistic alleles, with fluctuating values of selection and population sizes.

Invasion simulations

Modern coexistence theory has shown that coexistence is promoted by mechanisms that give species a population growth rate advantage over other species when they become rare (Chesson, 1982; 2003; Barabás *et al.*, 2018). Typically, one species is held at its *resident* state, as given by its steady-state abundances while the rare species is called the *invader*. In the context of alleles in a population, an allele is an *invader* when a mutation occurs that introduces that allele into a population in which it is absent (e.g., if in a population with only k alleles, a random mutation made one individual carry the j allele). Within sexually antagonistic selection, each allele has two pathways of invasion, depending on whether the mutation arises in a female or in a male. If an alleles' *invasion growth rate* (or the average instantaneous population growth rate when rare) is positive,

it buffers it against extinction, maintaining its persistence in the population. Coexistence, and hence polymorphism, occurs when both alleles have positive invasion growth rates.

To study the dynamics of sexually antagonistic alleles through this framework, we used the timeseries that captured the dynamics of our population model as a template to perform invasion simulations of both alleles. We allowed each allele to invade via two different pathways: males and females. We explored all potential combinations of each allele invading through a different pathway (e.g., allele j invading through males, and allele k invading through females, and so on). This yielded four types of invasion.

For each timestep in the timeseries, we performed simulations of the two alleles invading separately via their respective pathway. To simulate invasion, we set the density of the invading allele to one individual. For example, if allele j was invading via males, then we would set $n_{jm,i} = 1$ and $n_{jf,i} = 0$. Note that each invasion simulation was independent of the iteration that we used to generate the timeseries, therefore we denoted the initial timestep in an invasion simulation with the subscript i. We also set the resident allele, in this case k, to the corresponding value of the timeseries minus one individual, $n_{km,i} = N_{m,t} - 1$ and $n_{kf,i} = N_{f,t}$. Then, we iterated our model one timestep, $i + 1$, and calculated the logarithmic growth rate of j allele invading as:

$$r_j = \ln\left(\frac{n_{jm,i+1} + n_{jf,i+1}}{1}\right) \tag{11}$$

Correspondingly, the logarithmic growth rate of the k allele as a resident would be

given by:

$$r_k = \ln\left(\frac{n_{km,i+1} + n_{kf,i+1}}{n_{km,i} + n_{kf,i}}\right) \tag{12}$$

We treated each timestep of the timeseries independently, and hence we performed 500 invasion simulations. We then calculated, for each allele invading via a different pathway, its mean invasion growth rate as the average of the 500 invasion growth rates. We also calculated the mean growth rate of the resident allele as the average of the 500 resident growth rates. We determined alleles to be coexisting if both of alleles had positive mean invasion growth rates, which is often referred to as the mutual invasibility criterion (Barabás *et al.*, 2018).

Functional decompostion

Our invasion simulations tell us whether or not sexually antagonistic alleles can coexist in a determined point of the selection parameter space. However, we also quantified the relative contributions of fluctuating selection and population sizes into the predicted coexistence outcome. We did so by using an extension of MCT that provides the flexibility to analyze the contributions of different processes to coexistence using *functional decomposition* (Ellner *et al.*, 2016; 2019; Shoemaker *et al.*, 2020).

We applied the functional decomposition approach by breaking up the average growth rate of each allele into a null growth rate in the absences of fluctuations in all selected variables, a set of main effect terms that represent the effect of only one variable fluctuating, and a set of two-way interaction terms representing the effect of variables fluctuating simultaneously (Ellner *et al.*, 2019). In our simulations, this is a function of four variables:

the number of males in the population (N_m), the number of females in the population (N_f), the fitness of allele j in males (w_{jm}), and the fitness of allele k in females (w_{kf}). As an example, if only N_m and N_f were fluctuating, the growth rate of allele j when it is the invader at timestep t could be decomposed into:

$$r_{j,t}(N_m, N_f) = \mathcal{E}_j^0 + \mathcal{E}_j^{N_m} + \mathcal{E}_j^{N_f} + \mathcal{E}_j^{N_m N_f} \tag{13}$$

Where $\mathcal{E}^0$ is the null growth rate when N_m and N_f are set to their averages. Terms with superscripts represent the marginal effects of letting all superscripted variables vary while fixing all the other variables at their average values. For example, the term $\mathcal{E}^{N_m}$ expresses the contribution of fluctuations in N_m when N_f is at its average, without the contribution when both variables are set to their averages :

$$\mathcal{E}_j^{N_m} = r_{j,t}(N_m, \overline{N_f}) - \mathcal{E}_j^0 \tag{14}$$

If we average Eqn. 13 across the timesteps in our simulation, we get a partition of the average population growth rate into the variance–free growth rate, the main effects of variability in N_m, the main effects of variability in N_f, and the interaction between variability in N_m and N_f

$$\bar{r}_j = \mathcal{E}_j^0 + \overline{\mathcal{E}_j}^{N_m} + \overline{\mathcal{E}_j}^{N_f} + \overline{\mathcal{E}_j}^{N_m N_f} \tag{15}$$

However, in our simulations w_{jm} and w_{kf} also fluctuated, therefore the full functional decomposition of the growth rate of allele j as an invader is found in Table 2, as well as

a brief description of the meaning of each term. The implementation and interpretation of the functional decomposition of the invasion growth rates of each allele are identical to each other. Note that Table 2 does not include three of four–way interactions (e.g., $\overline{\mathcal{E}}_j^{N_m N_f w_{jm} w_{fk}}$). This is because in our simulations, we did not allow fluctuations in selection and population sizes to be correlated, therefore their effects are solely captured by the terms in Table 2. We calculated the value of each of the terms in Table 2 by performing another set of invasion simulations as described previously, but instead of allowing all variables to fluctuate, systematically setting the required variables to their means and subtracting the corresponding $\mathcal{E}$ values.

The functional decomposition approach further requires the *comparison* of each term, to understand if how it affects invaders and residents. This is because fluctuations can promote coexistence by helping whichever allele is rare, or they can hurt whichever allele is common. Therefore, to understand the role of each type of fluctuation, it is necessary to compare how it affects invader *and* resident growth rates. In the example presented in Eqn. 15, if allele j is invading, then allele k is at it's resident state and there exists an analogue decomposition of $\bar{r}_k$ with the exact same terms. Therefore we can express the difference between contributions of fluctuations in N_m as:

$$\Delta_j^{N_m} = \overline{\mathcal{E}}_j^{N_m} - \overline{\mathcal{E}}_k^{N_m} \tag{16}$$

If $\Delta_j^{N_m}$ is positive, then fluctuations in the male population benefit allele j when it is rare more than what they benefit k as a resident. If $\Delta_j^{N_m}$ is negative, then fluctuations

benefit k as a resident more than j as an invader, and if it is minimal, then fluctuations have an equal effect in j and k. Therefore, for each allele invading via a different pathway, we calculated 11 Δ values, one for each one of the $\mathcal{E}$ terms in Table 2. However, since the magnitude of each one of these values could vary considerably across the parameter space of selection, to make them comparable, we normalized each Δ value by dividing it by the square root of the sum of the squares of the 16 Δ values. For example, the normalized value of Eqn. 16 would be given by:

$$\delta_j^{N_m} = \frac{\Delta_j^{N_m}}{\sqrt{\sum_{d=1}^{11} (\mathbf{\Delta_d})^2}} \tag{17}$$

This normalization bounded δ values from -1 to 1.

3 Results

Our results showed that both fluctuations in selection and population sizes can substantially increase the expected genetic variability of sexually antagonistic alleles in a population. First, our results showed an increase in the proportion of allelic coexistence in the parameter space compared to classic theoretical expectations. As a baseline, we show in Fig. 1C the outcome of the control simulation, which matches previous findings that without fluctuations, alleles can coexist in only ≈ 0.38 of the selection parameter space (Connallon & Hall, 2018). Second, our results showed that each type of fluctuation contributed differently to the coexistence of alleles, and their contribution depended on the allele and sex in which invasion occurred. .

The effect of fluctuations in allelic coexistence

When only population sizes fluctuated, the average proportion of coexistence increased with the effect size of fluctuations when fluctuations were large enough (Fig. 1A). Fluctuations with small effect sizes ($\sigma_g < 20$) either decreased or matched the average proportion of the parameter space of allelic coexistence compared to the control simulation. Note that an effect size of $\sigma_g = 20$ means that fluctuations increased or decreased population sizes approximately 10% in each timestep. Above this value, as the effect size of fluctuations increased so did the average proportion of the parameter space where alleles could coexist, reaching up to ≈ 0.50 (Fig. 1A). Importantly, the average proportion of allelic coexistence was highest when fluctuations were negatively correlated (Fig. 1A).

When only selection fluctuated, the average proportion of coexistence increased non-linearly as the effect size of fluctuations increased (Fig. 1B). Note, however, that simulations with small effect sizes ($\sigma_w < 0.2$) yielded identical results as the control simulation (Fig. 1B). Increases in the effect size of fluctuations after this value dramatically increased the average proportion of the parameter space where alleles could coexist, reaching up to ≈ 0.90 (Fig. 1B). In contrast to fluctuations in population sizes, the effect of fluctuations in selection was the highest when fluctuations were positively correlated (Fig. 1B).

When *both* population sizes and selection fluctuated, large fluctuations increased the average proportion of allelic coexistence as the effect size of fluctuations increased (Fig. 2). These increments were greater in magnitude when $\rho_g = -0.75$ and $\rho_w = 0.75$ (Fig. 2). Notably, the effects of fluctuations in selection and population sizes were not synergic.

Indeed, at high fluctuations ($\sigma_g = 70$ or $\sigma_w = 0.9$), the average proportion of coexistence was higher when only selection fluctuated compared to when both selection and population sizes were simultaneously fluctuating (Fig. 2).

The relative contribution of fluctuations

Despite that fluctuations tended to increase the average proportion of coexistence, not all fluctuations contributed positively to allelic coexistence. To illustrate this point, we show in Fig. 4A the outcome of one of our simulations (white square in Fig. 2). In this simulation, the proportion of coexistence was 0.8, more than double the parameter space compared to the control simulation (Fig. 1C). This increase in the proportion of coexistence is because in parts of the parameter space where selection would typically favor the fixation of one of the alleles, fluctuations in population sizes and fitness values allow their coexistence (grey area in Fig. 1C compared to the grey area in Fig. 4A). However, note that there are also parts of the parameter space where coexistence is lost compared to the control simulation (Fig. 1C compared to Fig. 4A).

Simulations in which population sizes fluctuated, yielded both coexistence gains and losses in the selection parameter space (Fig. 4A). In contrast, simulations in which only selection fluctuated, resulted in increases of allelic coexistence (Fig. S1 Supporting Information). This was the main reason why the maximum proportion of coexistence was not achieved when both types of fluctuations were operating simultaneously (Fig. 2). Coexistence gains and losses in the parameter space are the result of the sum of relative contributions of each type of fluctuation. We show in Fig. 4B the δ values that contributed

to the coexistence outcomes shown in Fig. 4A.

Our functional decomposition approach showed that the same type of fluctuation can benefit one allele when it is rare while also creating a disadvantage for the invasion of the other allele. For example, δ^{N_m} benefited allele j as an invader but contributed negatively when allele k was the invader (Fig. 4B). In contrast, δ^{N_f} had the opposite effect (Fig. 4B). The relative contribution of fluctuations was consintent in the selection parameter space for each allele: each δ value was either positive and neutral, or negative and neutral, except for δ^0 which could have both negative and positive contributions for both alleles (Fig. 4B). Ultimately, allelic coexistence only happened in parts of the parameter space where alleles had a positive invasion growth rate, which was achieved as long as positive contributions of δ outweighed the negative contributions. As an example, we highlight in (Fig. 4B) a point in the parameter space where coexistence is lost compared to the control simulation. This loss was driven mainly by a strong negative contribution of δ^0 to the invasion growth rate of allele k.

The patterns shown in Fig. 4B remained when we examined the relative contributions of fluctuations in different invasion scenarios and across replicates (Fig. 5). Our results showed that the relative contribution of fluctuations in population sizes depended on the sex where invasion occurred. The relative contribution of fluctuations in the male population, δ^{N_m}, was positive for both j and k alleles when the mutation that introduced them to the population happened in males and negative if invasion occurred via females (Fig. 5A).The opposite pattern was exhibited by δ^{N_m} (Fig. 5A). The correlation between fluctuations ρ_g determined the effect of $\delta^{N_m N_f}$: it contributed positively to both alleles

invading via both pathways when fluctuations were negatively correlated, it had a negligible effect when fluctuations were not correlated, and it had a negative effect when fluctuations were positively correlated (Fig. 5A).

In contrast, the effect of fluctuations in selection was independent of the sex where invasion occurred. The values of $\delta^{w_{jm}}$ were positive for the k allele, and negative for the j allele, regardless of the via of invasion (Fig. 5B). The opposite pattern was exhibited by $\delta^{w_{kf}}$ (Fig. 5B). Thus, fluctuations in selection always benefited the allele that selection did not affect. Finally, the correlation between fluctuations determined the effect of $\delta^{w_{jm}w_{kf}}$; a negative correlation between fluctuations caused $\delta^{w_{jm}w_{kf}}$ to have negative contributions, . no correlation between fluctuations caused $\delta^{w_{jm}w_{kf}}$ to have a negligible effect, and a positive correlation between fluctuations made $\delta^{w_{jm}w_{kf}}$ to have positive contributions to the growth rates of both alleles (Fig. 5B).

The effect of sex ratios

As we show in Fig. 4, fluctuations in population sizes can in some instances, cause the loss of coexistence in the parameter space. These losses were driven by stochastic changes of the value δ^0 can take (Fig. 4B). Note that δ^0 captured the effect of fluctuations when they were set to their averages. In the control simulation δ^0 captured exclusively the effect of selection (Fig. 6A). Incorporating fluctuations in selection do not fundamentally change the value of δ^0 compared to the control simulation (Fig. 6A). However, fluctuations in the population size of the male and female populations stochastically change the values of δ^0 compared to the control simulations (Fig. 6A). These stochastic contributions were

caused by changes in the sex ratios in our simulations which were not captured by the rest δ values and explain the losses of coexistence in the parameter space (Fig. 6A).

Figures and tables

Table 1: Parameters used in our simulations to control the effect size of fluctuations in population sizes (σ_g) and selection values (σ_w), as well as their respecitve correlations (ρ_g and ρ_w). We ran ten replicates for each one of the factorial combinations of the following parameters.

Parameter	Values	Description
σ_w	0.001, 0.1, 0.3, 0.5, 0.7, 0.9	Effect size of fluctuations in fitness values
σ_g	0.001, 1, 10, 20, 30, 50	Effect size of fluctuations in population sizes
ρ_w	-0.75, 0, 0.75	Correlation between fluctuations in fitness values
ρ_g	-0.75, 0, 0.75	Correlation between fluctuation in population sizes

Table 2: Functional decomposition of the growth rate of allele j. As we show in Eqn. 15, each term captures the contribution of fluctuations to an alleles' invasion growth rate.

Term	Formula	Meaning
$\mathcal{E}_j^0$	$\overline{r_j}(\overline{N_m}, \overline{N_f}, \overline{w_{jm}}, \overline{w_{kf}})$	Growth rate at mean population size and fitness values.
$\overline{\mathcal{E}}_j^{N_m}$	$\overline{r}_j(N_m \overline{N_f}, \overline{w_{jm}}, \overline{w_{kf}}) - \mathcal{E}_j^0$	Main effect of fluctuations in N_m
$\overline{\mathcal{E}}_j^{N_f}$	$\overline{r_j}(\overline{N_m}, N_f, \overline{w_{jm}}, \overline{w_{kf}}) - \mathcal{E}_j^0$	Main effect of fluctuations in N_f
$\overline{\mathcal{E}}_j^{w_{jm}}$	$\overline{r_j}(\overline{N_m}, \overline{N_f}, w_{jm}, \overline{w_{kf}}) - \mathcal{E}_j^0$	Main effect of fluctuations in w_{jm}
$\overline{\mathcal{E}}_j^{w_{kf}}$	$\overline{r_j}(\overline{N_m}, \overline{N_f}, \overline{w_{jm}}, w_{kf}) - \mathcal{E}_j^0$	Main effect of fluctuations in w_{kf}
$\overline{\mathcal{E}}_j^{N_m, N_f}$	$\overline{r_j}(N_m, N_f, \overline{w_{jm}}, \overline{w_{kf}}) - [\mathcal{E}_j^0 + \overline{\mathcal{E}}_j^{N_m} + \overline{\mathcal{E}}_j^{N_f}]$	Interaction of fluctuations in N_m and N_f
$\overline{\mathcal{E}}_j^{w_{jm}, w_{kf}}$	$\overline{r_j}(\overline{N_m}, \overline{N_f}, w_{jm}, w_{kf}) - [\mathcal{E}_j^0 + \overline{\mathcal{E}}_j^{w_{jm}} + \overline{\mathcal{E}}_j^{w_{kf}}]$	Interaction of fluctuations in w_{jm} and w_{kf}
$\overline{\mathcal{E}}_j^{N_m w_{jm}}$	$\overline{r_j}(N_m, \overline{N_f}, w_{jm}, \overline{w_{kf}}) - [\mathcal{E}_j^0 + \overline{\mathcal{E}}_j^{N_m} + \overline{\mathcal{E}}_j^{w_{jm}}]$	Interaction of fluctuations in N_m and w_{jm}
$\overline{\mathcal{E}}_j^{N_m w_{kf}}$	$\overline{r_j}(N_m, \overline{N_f}, \overline{w_{jm}}, w_{kf}) - [\mathcal{E}_j^0 + \overline{\mathcal{E}}_j^{N_m} + \overline{\mathcal{E}}_j^{w_{kf}}]$	Interaction of fluctuations in N_m and w_{kf}
$\overline{\mathcal{E}}_j^{N_f w_{jm}}$	$\overline{r_j}(\overline{N_m}, N_f, w_{jm}, \overline{w_{kf}}) - [\mathcal{E}_j^0 + \overline{\mathcal{E}}_j^{N_f} + \overline{\mathcal{E}}_j^{w_{jm}}]$	Interaction of variation in N_f and w_{jm}
$\overline{\mathcal{E}}_j^{N_f w_{fk}}$	$\overline{r_j}(\overline{N_m}, N_f, \overline{w_{jm}}, w_{kf}) - [\mathcal{E}_j^0 + \overline{\mathcal{E}}_j^{N_f} + \overline{\mathcal{E}}_j^{w_{kf}}]$	Interaction of fluctuations N_f and w_{kf}

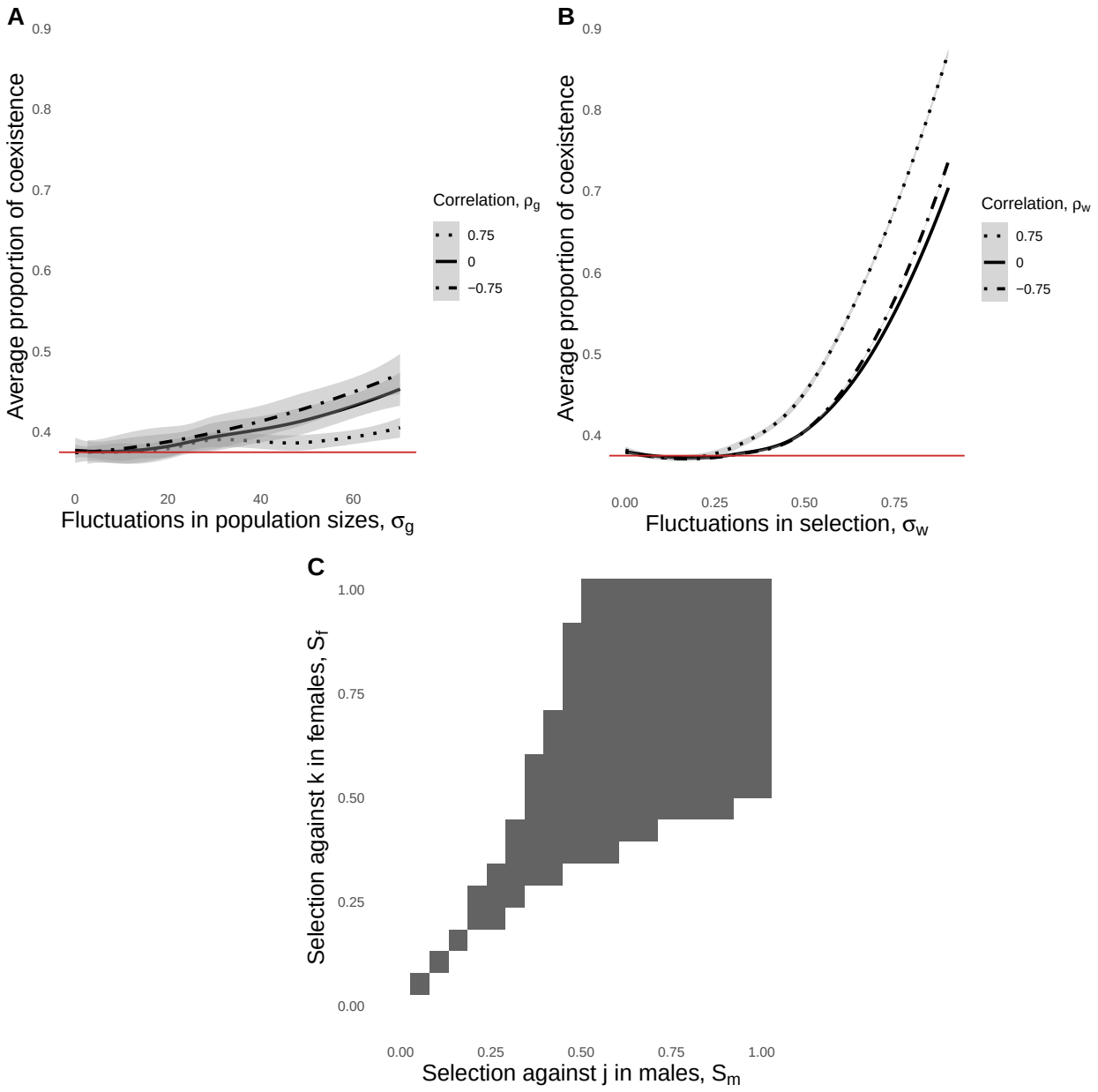

Figure 1: Changes in the proportion of coexistence as a function of fluctuations. In A) we show the results of simulations in which only population sizes fluctuated (i.e., simulations in which $\sigma_w = 0.001$ and $\rho_w = 0$). We show how the average proportion of coexistence, for all of the different invasion scenarios and replicates, changed as a function of the effect size of fluctuations in population sizes with black lines. We denoted the correlation between fluctuations in our simulations with different line types and displayed confident intervals around the average with shaded areas. The solid red line corresponds to the proportion of coexistence in the control simulation. In B) we show the same results for simulations where only selection fluctuated (i.e., simulations in which $\sigma_g = 0.001$ and $\rho_g = 0$). Finally, in C) we show the results of the control simulation in the selection parameter space. Grey areas denote points in the parameter space where selection maintains both alleles in a population, which amount to ≈ 0.38 of the selection parameter space, while white areas show competitive exclusion.

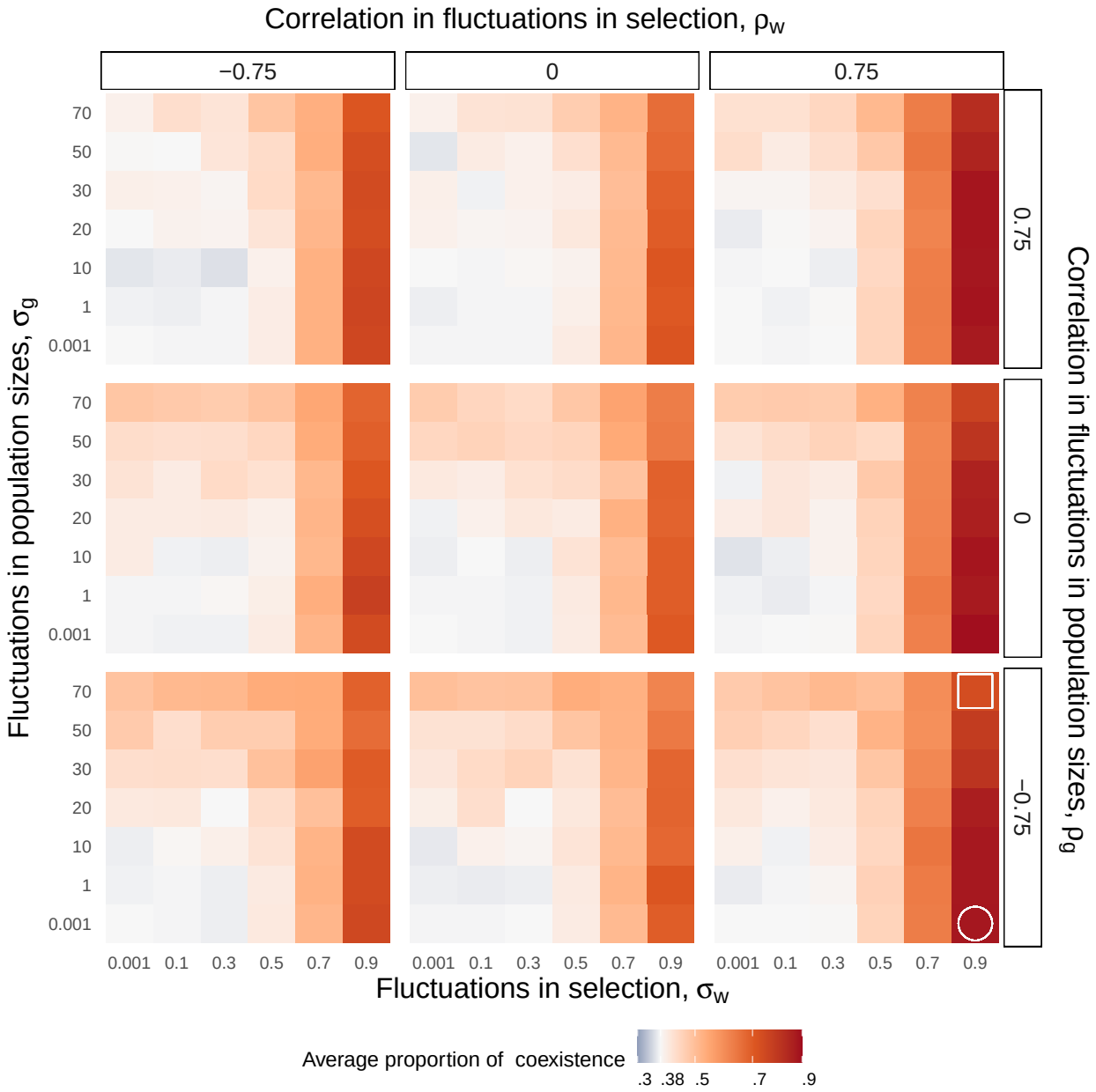

Figure 2: Average proportion of coexistence for different parameter combinations. We show, for all factorial combinations of σ_g, σ_w, ρ_g and ρ_w, the average proportion of coexistence of in our simulations. Each panel corresponds to a different combination of correlations between fluctuations. Labels on top indicate the correlation between fluctuations in selection ρ_w, while labels on the right show the correlation in fluctuations between fluctuations in population sizes ρ_g. As a basis of comparison, we show the expected proportion of coexistence (0.38) as the midpoint in our color scheme. Finally, the white square and circle at the bottom left panel are references to simulations we show in detail in later figures.

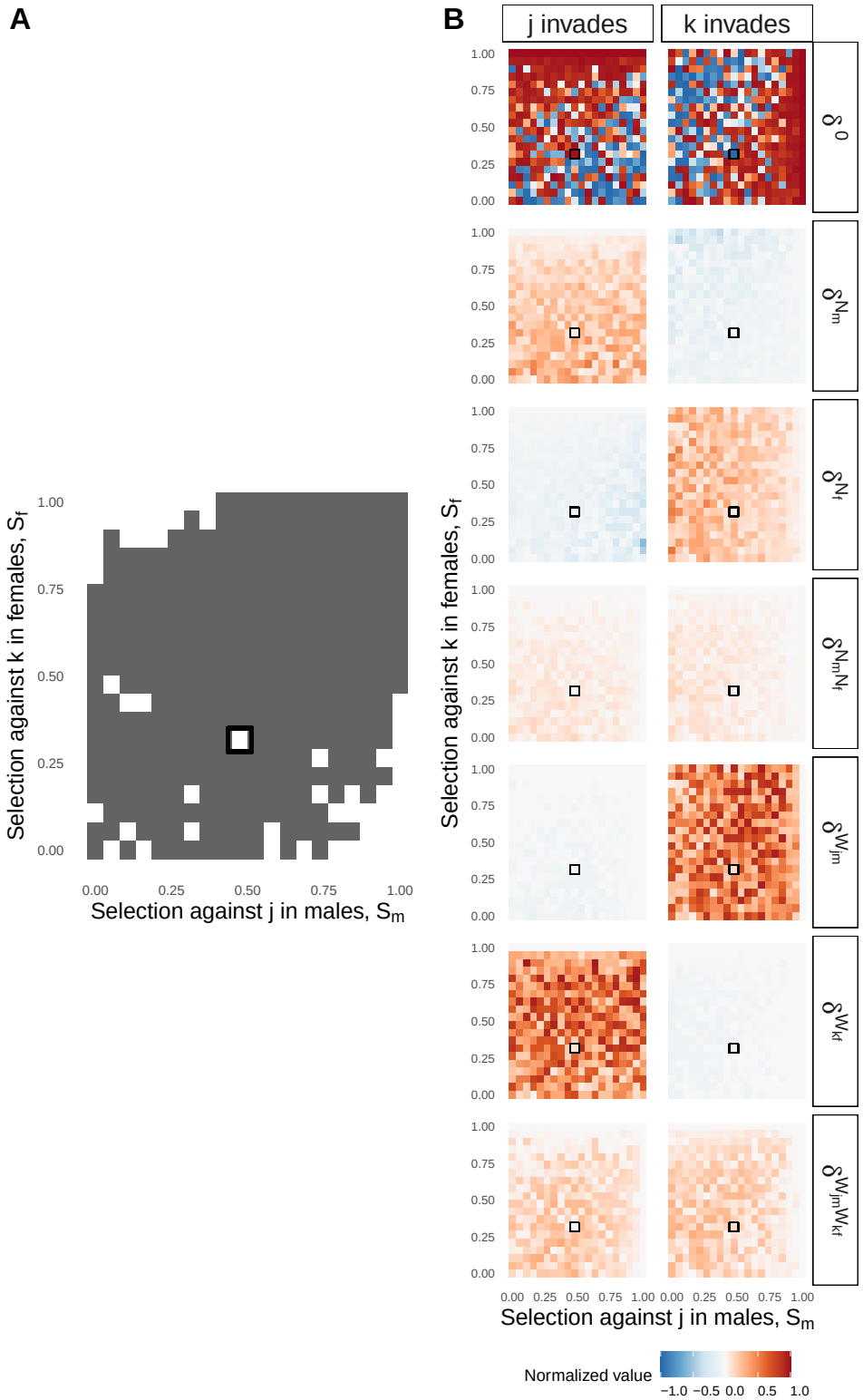

Figure 3: Coexistence outcomes and functional decomposition of one simulation. We show in A) for one of the replicates highlighted with a white square in Fig. 2 ($\sigma_g = 70$, $\sigma_w = 0.9$, $\rho_g = -0.75$ and $\rho_{w=0.75}$,) the coexistence outcomes when j invades via females and k invades via males. Grey areas denote points in the parameter space where alleles can coexist, while white areas are points where at least one allele does not have a positive invasion growth rate. We highlight in black a point in the parameter space where coexistence is lost compared to the control simulation. In B) we show for the same simulation, the functional decomposition of each allele across the parameter space of selection. The highlighted black points correspond to the same point shown in A).

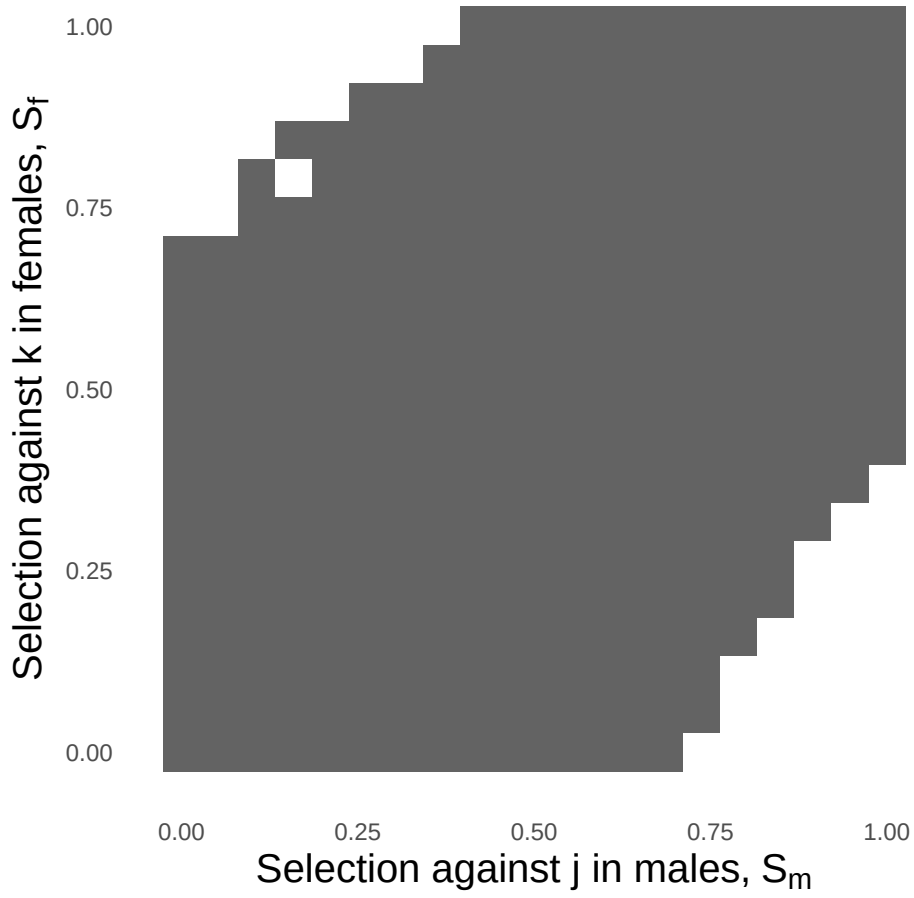

Figure 4: This figure will go in the Supporting Information. We show the coexistence outcomes for one of the replicates highlighted with a white circle in Fig. 2 ($\sigma_g = 70$, $\sigma_w = 0.9$, $\rho_g = -0.75$ and $\rho_{w=0.75}$,) when j invades via females and k invades via males. Grey areas denote points in the parameter space where alleles can coexist, while white areas are points where at least one allele does not have a positive invasion growth rate.

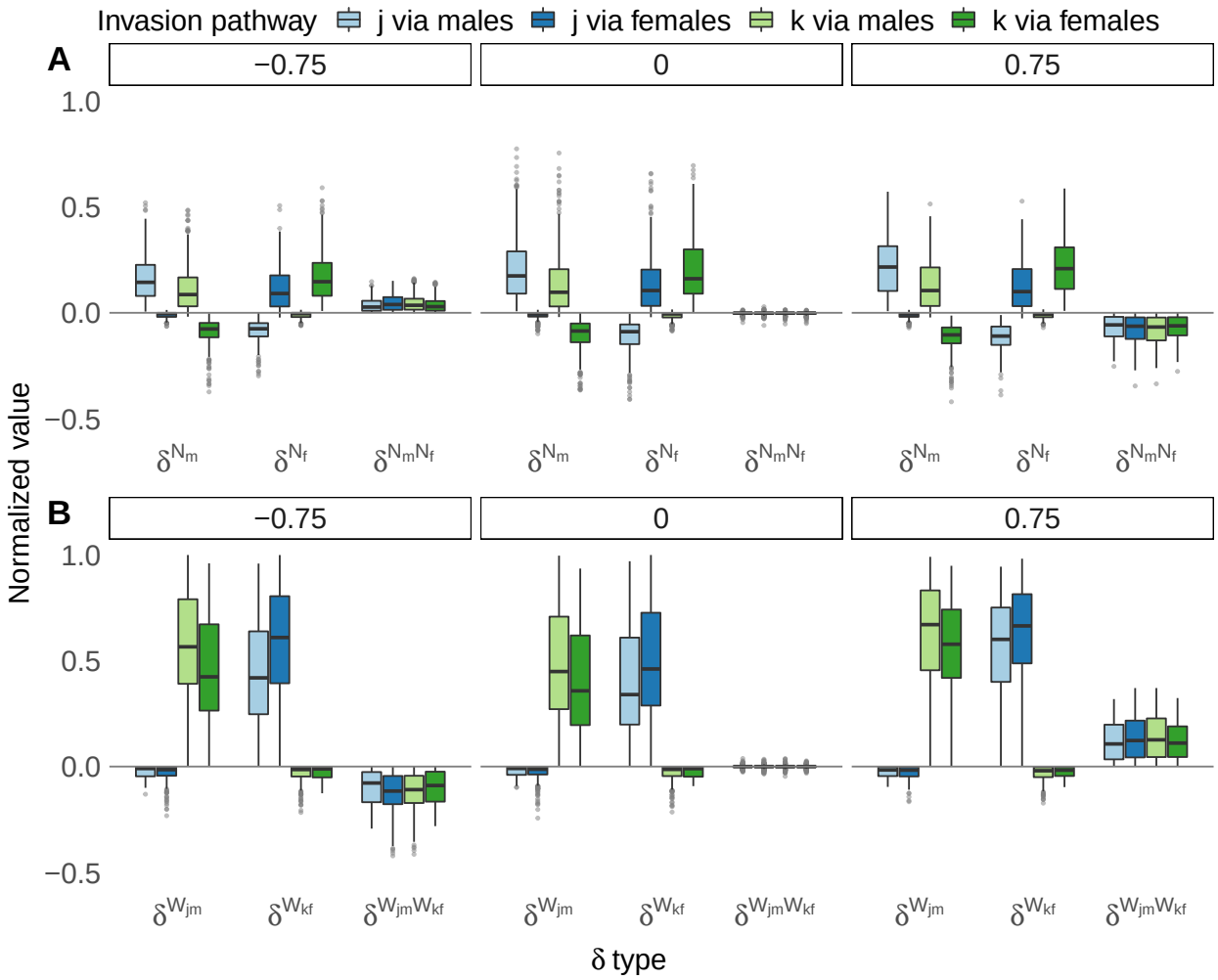

Figure 5: Boxplots of δ values. In A) we show the box plots of δ values that capture the relative contributions of fluctuations in population sizes, for all of the replicates in our simulation in which $\sigma_g = 70$ and $\sigma_w = 0.001$. Labels on top indicate the correlation between fluctuations in population sizes, ρ_g. Each color corresponds to a different allele and invasion pathway in our simulations. In B) we show the box plots of δ values that capture the contributions of fluctuations in selection, for all of the replicates in our simulation in which $\sigma_w = 0.9$ and $\sigma_g = 0.001$. Labels on top indicate the correlation between fluctuations in selection, ρ_w, with the same color nomenclature as in A). Each box plot extends from the first to third quantiles of the corresponding posterior distribution of parameter values, and the line inside the the box indicates the median. The upper whisker extends to the largest value no further than 1.5 times the inter-quantile range (IQR, or the distance between the first and third quartiles); the lower whisker extends to the smallest value at most 1.5 times the IQR. Data beyond the end of the whiskers are determined to be outliers and are plotted individually with solid grey points.

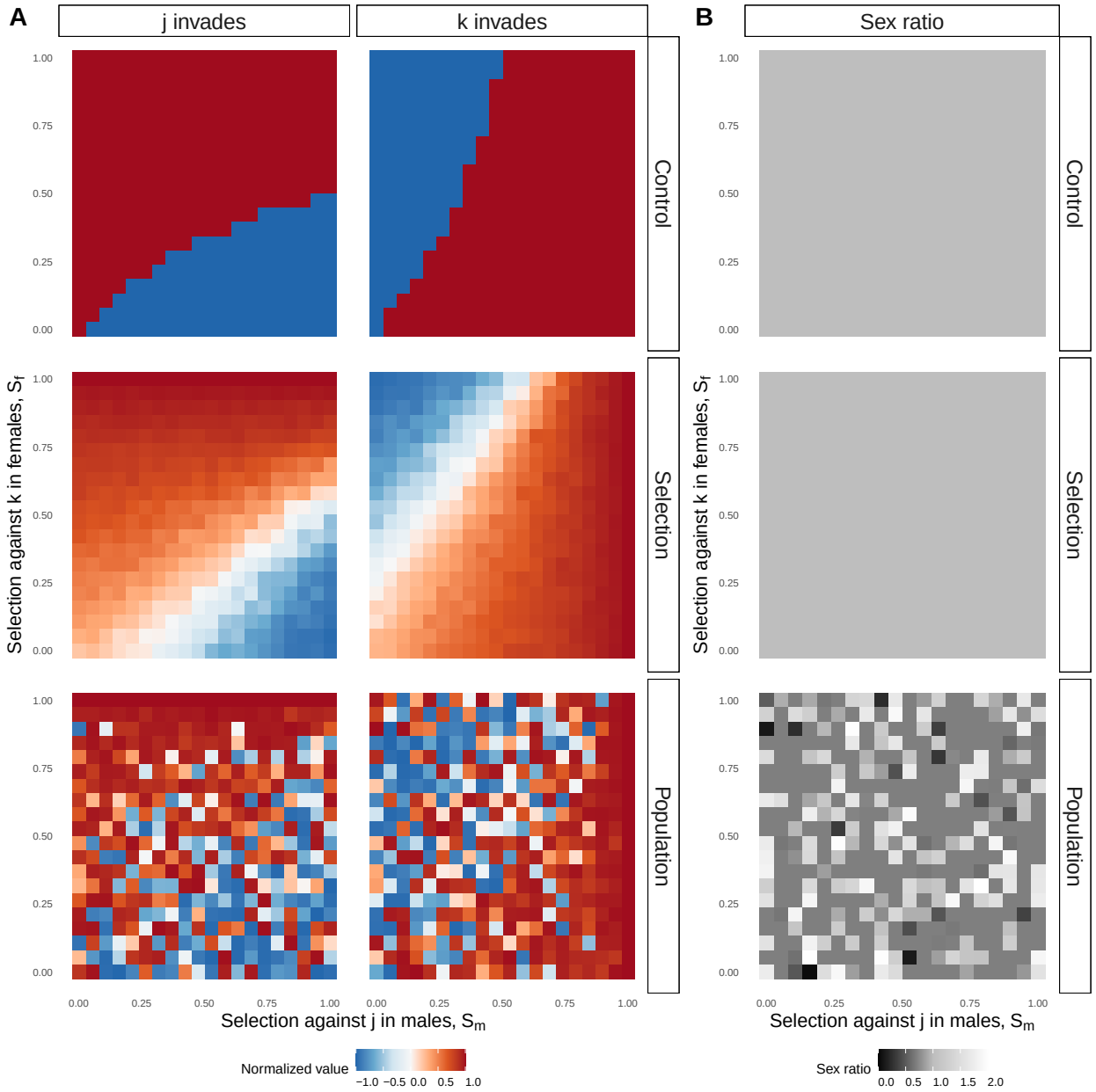

Figure 6: The relationship between δ^0 and sex ratios. In A) we show the values of δ^0 accross the selection parameter space for different types of simulations when j invades via males and k invades via females. Each pannel corresponds to an allele invading a population in a replicate of different simulations, as labels on the right indicate: Control denotes the control simulation, Selection denotes a simulation where $\sigma_w = 0.9$ and $\sigma_g = 0.001$, and Population indicates a simulation where $\sigma_w = 0.001$ and $\sigma_g = 70$. For simplicity we kept both correlations equal to zero. In B), we show for the same replicates shown in A), the sex ratios, calculated as $\frac{N_f}{N_m}$, accross the selection parameter space.

References

Barabás, G., D'Andrea, R. & Stump, S.M. (2018). Chesson's coexistence theory. *Ecological Monographs*, 88, 277–303.

Chesson, P. (1994). Multispecies competition in variable environments. *Theoretical population biology*, 45, 227–276.

Chesson, P. (2000a). General theory of competitive coexistence in spatially-varying environments. *Theoretical Population Biology*, 58, 211–237.

Chesson, P. (2000b). Mechanisms of maintenance of species diversity. *Annual review of Ecology and Systematics*, 31, 343–366.

Chesson, P. (2003). Quantifying and testing coexistence mechanisms arising from recruitment fluctuations. *Theoretical Population Biology*, 64, 345–357.

Chesson, P.L. (1982). The stabilizing effect of a random environment. *Journal of Mathematical Biology*, 15, 1–36.

Connallon, T. & Hall, M.D. (2018). Environmental changes and sexually antagonistic selection. *eLS*, pp. 1–7.

Connallon, T., Sharma, S. & Olito, C. (2018). Evolutionary Consequences of Sex-Specific Selection in Variable Environments: Four Simple Models Reveal Diverse Evolutionary Outcomes. *The American Naturalist*, 193, 93–105.

Ellner, S. & Hairston Jr, N.G. (1994). Role of overlapping generations in maintaining genetic variation in a fluctuating environment. *The American Naturalist*, 143, 403–417.

Ellner, S. & Sasaki, A. (1996). Patterns of genetic polymorphism maintained by fluctuating selection with overlapping generations. *theoretical population biology*, 50, 31–65.

Ellner, S.P., Snyder, R.E. & Adler, P.B. (2016). How to quantify the temporal storage effect using simulations instead of math. *Ecology letters*, 19, 1333–1342.

Ellner, S.P., Snyder, R.E., Adler, P.B. & Hooker, G. (2019). An expanded modern coexistence theory for empirical applications. *Ecology Letters*, 22, 3–18.

Gavrilets, S. (2014). Is sexual conflict an "engine of speciation"? *Cold Spring Harbor perspectives in biology*, 6, a017723.

Hedrick, P.W. (1974). Genetic variation in a heterogeneous environment. i. temporal heterogeneity and the absolute dominance model. *Genetics*, 78, 757–770.

Hedrick, P.W. (1986). Genetic polymorphism in heterogeneous environments: a decade later. *Annual review of ecology and systematics*, 17, 535–566.

Immler, S., Arnqvist, G. & Otto, S.P. (2012). Ploidally antagonistic selection maintains stable genetic polymorphism. *Evolution: International Journal of Organic Evolution*, 66, 55–65.

Kidwell, J., Clegg, M., Stewart, F. & Prout, T. (1977). Regions of stable equilibria for models of differential selection in the two sexes under random mating. *Genetics*, 85, 171–183.

Mitchell-Olds, T., Willis, J.H. & Goldstein, D.B. (2007). Which evolutionary processes influence natural genetic variation for phenotypic traits? *Nature Reviews Genetics*, 8, 845–856.

Nunney, L. (2002). The effective size of annual plant populations: the interaction of a seed bank with fluctuating population size in maintaining genetic variation. *The American Naturalist*, 160, 195–204.

Pamilo, P. (1979). Genic variation at sex-linked loci: Quantification of regular selection models. *Hereditas*, 91, 129–133.

Pemberton, J., Smith, J., Coulson, T.N., Marshall, T.C., Slate, J., Paterson, S., Albon, S., Clutton-Brock, T.H. & Sneath, P.H.A. (1996). The maintenance of genetic polymorphism in small island populations: large mammals in the hebrides. *Philosophical Transactions of the Royal Society of London. Series B: Biological Sciences*, 351, 745–752.

Reinhold, K. (2000). Maintenance of a genetic polymorphism by fluctuating selection on sex-limited traits. *Journal of Evolutionary Biology*, 13, 1009–1014.

Shoemaker, L.G., Barner, A.K., Bittleston, L.S. & Teufel, A.I. (2020). Quantifying the relative importance of variation in predation and the environment for species coexistence. *Ecology letters*, 23, 939–950.

Walsh, B. & Lynch, M. (2018). *Evolution and Selection of Quantitative Traits*. OUP Oxford.

Wright, S. (1942). Statistical genetics and evolution. *Bulletin of the American Mathematical Society*, 48, 223–246.